# Classical Theory of the Pair Distribution Function of Plasmas*

HUGH E. DEWITT
*Lawrence Radiation Laboratory, University of California, Livermore, California*
(Received 17 May 1965)

The diagrammatic method used by Abe to obtain the Helmholtz free energy of the classical electron gas is used to derive the pair distribution function beyond the Debye-Hückel result. The calculation can be done systematically either in configuration space or wave-number space and is carried out exactly to $O(\Lambda^2)$ where $\Lambda=\frac{1}{4}\pi\rho\lambda_D^3$ is the classical plasma parameter. It is shown that $g(r)$ has the form $g(r)=e^{-\beta u_s}[1+g_2^b(r)+g_2^c(r)]$, where $u_s=(e^2/r)\exp(-r/\lambda_D)$ is the Debye screened potential, and $g_2^b$ and $g_2^c$ are functions of $r/\lambda_D$ which are evaluated analytically to $O(\Lambda^2)$. For the region $\beta e^2<r<\lambda_D$ the correction in brackets multiplying the Boltzmann factor $\exp(-\beta u_s)$ is less than 1. A surprising result is that for $r\gg\lambda_D$ the linear Debye-Hückel theory does not correctly describe the disappearance of particle correlations, and instead the correction function $g_2^c$ dominates. As $r\to\infty$ it is found that $g(r)-1\sim\frac{1}{8}(\ln 3)\Lambda^2\exp(-r/\lambda_D)$.

## I. INTRODUCTION

THE classical Debye-Hückel theory[1] gives a familiar, useful, and simple result for the distribution of a pair of particles of charge $z_1e$ and $z_2e$ at a distance $r$ apart:

$$g(r)=1-(z_1z_2\beta e^2/r)\exp(-r/\lambda_D)=1-\beta z_1z_2u_s(r), \quad (1)$$

where $u_s(r)$ is the static screened Coulomb potential with $\lambda_D=(4\pi\beta e^2\sum z_\alpha^2\rho_\alpha)^{-1/2}$. The Debye-Hückel derivation of this expression is valid when $\beta u_s(r)<1$, and hence for particle separations greater than the average distance of closest approach $r>\beta e^2$. For $r<\beta e^2$ Eq. (1) gives a meaningless negative result for $g(r)$. Nevertheless, in spite of this difficulty for small $r$, the Debye-Hückel result is useful since it describes the screening out of particle correlations at distances such that $r\sim\lambda_D$. Also Eq. (1) may be used to obtain the correct leading order result for the Coulombic interaction energy valid at high temperature and low density, i.e., when $\beta e^2/\lambda_D<1$. The purpose of this paper is to systematically calculate corrections to the Debye-Hückel expression and obtain results for $g(r)$ that will be valid for short distances $r\sim\beta e^2$. In the classical theory the short-distance difficulty of Eq. (1) is not worrisome since it is understood that the actual behavior as $r\to 0$ must be described by the Boltzmann factor,

$$g(r)\approx\exp(-z_1z_2e^2/r).$$

For charges of like sign, electron-electron and ion-ion pairs, the Boltzmann factor vanishes strongly as $r\to 0$. For charges of unlike sign the Boltzmann factor diverges badly as $r\to 0$ and gives the classical catastrophe of the attractive Coulomb force causing point particles to collapse together. Quantum mechanics through the uncertainty principle saves this situation since the point charges have a finite extension, the thermal de Broglie wavelength $\lambda\!\!\!^{-}_{12}=\hbar/(2m_{12}kT)^{1/2}$, and the classical Boltzmann factor applies only for $r>\lambda\!\!\!^{-}_{12}$. In this paper we are mainly interested in the case of repulsion so that classical theory may be assumed down to $r=0$. Thus the work which follows applies primarily to the electron gas in a continuous positive background, and to the ion-ion pair distribution function in real plasmas for which usually $\lambda\!\!\!^{-}_{ii}<\beta e^2$ because of the large mass of the ions. The results here will also apply to electron-electron and electron-ion pairs for distances greater than the appropriate thermal de Broglie wavelength.

The nodal expansion of Meeron[2] and Friedman[3] as applied to the classical electron gas by Abe[4] provides a systematic perturbation expansion of the partition function from which one obtains the Helmholtz free energy

$$\beta(F-F_0)=-N\left\{\frac{\Lambda}{3}+\frac{\Lambda^2}{12}(\ln\Lambda-D_c)+\frac{\Lambda^3}{12}\ln\Lambda\cdots\right\}, \quad (2)$$

where $\Lambda=\beta e^2/\lambda_D=1/4\pi\rho\lambda_D^3$, and $D_c=\ln 3-2C+11/6$ with $C=0.5772$. The term of first order in $\Lambda$ is the Debye-Hückel result obtained from the ring diagrams and the higher order terms exhibited in Eq. (2) are obtained from the watermelon diagrams or ladder diagrams in the quantum theory. Beginning with $O(\Lambda^3)$ more complicated diagrams contribute, namely, watermelons connecting clusters of three and more particles. The same diagrammatic methods used to obtain Eq. (2) may with more work be used to calculate $g(r)$. A test of the results is that the appropriate integral must give back the known exact results for the free energy.

Recently Frieman and Book[5] have suggested a corrected form of $g(r)$, namely:

$$g(r)\approx 1-\beta u_s(r)+e^{-\beta e^2/r}-(1-\beta e^2/r)$$
$$=(\Lambda/x)(1-e^{-x})+e^{-\Lambda/x}, \quad x=r/\lambda_D. \quad (3)$$

This result is an improvement over the Debye-Hückel result, but is nevertheless too crude since a calculation

* Work performed under the auspices of the U. S. Atomic Energy Commission.

[1] For a modern treatment of the Debye-Hückel theory as applied to fully ionized gases see L. D. Landau and E. M. Lifshitz, *Statistical Physics* (Pergamon Press, Inc., New York, 1958), pp. 229–233.

[2] E. Meeron, Phys. Fluids **1**, 139 (1958).

[3] H. L. Friedman, *Ionic Solution Theory Based on Cluster Expansion Methods* (Interscience Publishers, Inc., New York, 1962).

[4] R. Abe, Progr. Theoret. Phys. (Kyoto) **22**, 213 (1959).

[5] E. A. Frieman and D. L. Book, Phys. Fluids **6**, 1700 (1963).

of the free energy with it gives a logarithmically divergent result. The Frieman-Book expression becomes more reasonable if the screened potential $u_s(r)$ is used in place of $e^2/r$ in Eq. (3); thus one obtains

$$g(r)\approx\exp(-\beta u_s)=\exp(-(\Lambda/x)e^{-x}). \tag{4}$$

We will call Eq. (4) the nonlinear Debye-Hückel pair distribution. It was considered by Carley[6] and compared numerically with the hypernetted chain approximation and the Percus-Yevick results. The presence of screening in Eq. (4) removes the logarithmic divergence in the calculation of $\beta F$ that one has with Eq. (3). The $O(\Lambda^2\ln\Lambda)$ term in Eq. (2) is obtained correctly, but the terms of $O(\Lambda^2)$ and $O(\Lambda^3\ln\Lambda)$ are incorrect.

Since it is useful to connect expressions for $g(r)$ with known exact results for the free energy, we begin with the diagrammatic expansion of $\beta F$ and use it to generate the appropriate diagrams for $g(r)$. For this purpose some formal relations should be noted. The free energy is connected to the pair distribution function by the relation

$$\beta(F-F_0)=\tfrac{1}{2}N\rho\int_0^1\frac{dc}{c}\int d^3r\,\beta u_c(r)g_c(r), \tag{5}$$

where $c$ is a measure of the coupling constant. Thus for the Coulomb potential we have $e'^2=ce^2$, the Debye charging process. The internal energy is a more convenient quantity, namely,

$$\begin{aligned}\beta(E-E_0)&=c(\partial/\partial c)\beta(F-F_0)_c\\&=\tfrac{1}{2}N\rho\int d^3r\,\beta u(r)g(r).\end{aligned} \tag{6}$$

If both $u(r)$ and $g(r)$ have Fourier transforms, then Eq. (6) may also be written as

$$\beta(E-E_0)=\tfrac{1}{2}N^2\int\frac{Vd^3k}{(2\pi)^3}\beta u(k)g(k), \tag{7}$$

where

$$u(k)=V^{-1}\int d^3r\,e^{i\mathbf{k}\cdot\mathbf{r}}u(r).$$

In the Abe calculation of the free energy of the electron gas the result is of the form

$$\beta(F-F_0)=-N\{S_{\text{ring}}(\Lambda)+\sum_{n=2}S_n(\Lambda)\}, \tag{8}$$

where the summation $n$ is over clusters of nodal point particles, namely, particles with three and more interactions ending on them. The evaluation of $S_2(\Lambda)$ gives Eq. (2); $S_3(\Lambda)$ and $S_4(\Lambda)$ begin with $O(\Lambda^3)$. In this expansion all simple chains of Coulomb interactions

[6] D. D. Carley, Phys. Rev. 131, 1406 (1963).

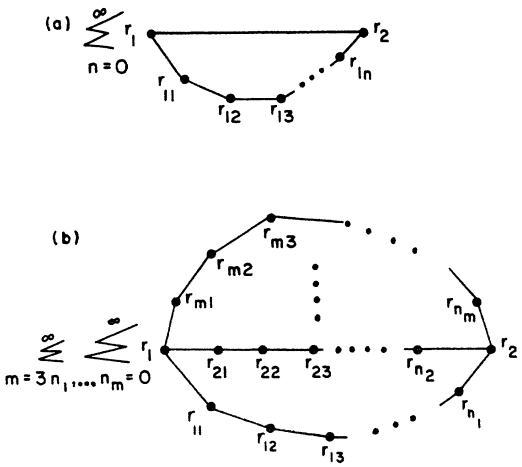


FIG. 1. Diagrams contributing to the lowest order results for the Helmholtz free energy. In configuration space every particle coordinate is integrated over all space. In (a) the ring diagrams are shown as a modification of second-order perturbation theory. In (b) the Abe watermelon diagrams are shown. Here one sums not only chains of Coulomb interactions, but also the number of screened lines. Points $r_1$ and $r_2$ are the nodal points.

are summed to produce screened Coulomb potentials. We can also write the following relationship which corresponds to Eq. (8)

$$g(r)=1+g_{\text{ring}}(\Lambda,x)+\sum_{n=2}g_n(\Lambda,x),\quad x=r/\lambda_D, \tag{9}$$

where $g_n(\Lambda,x)$, when substituted into the free-energy expression Eq. (5), gives $S_n(\Lambda)$ in Eq. (8). Similarly $g_n(\Lambda,\kappa)$ with $\kappa=k\lambda_D$ will denote the Fourier transform of $g_n(\Lambda,x)$ that goes into Eq. (7) to give the internal energy.

## II. DIAGRAMMATIC EXPANSION OF THE PAIR DISTRIBUTION FUNCTION

Although the perturbation expansion of the pair distribution function expressed by a sequence of diagrams may be written down without reference to the Helmholtz free energy, it seems convenient to use the diagrammatic expansion of the free energy to generate the expansion for $g(r)$. In the theory of the electron gas one must first, by adding up the appropriate groups of diagrams, remove the various divergencies that appear due to the long- and short-distance behavior of the $1/r$ potential. The sequence of operations is shown in Fig. 1. First one corrects the linear divergence of second-order perturbation theory by adding the ring diagrams. The long-distance logarithmic divergence of the third order is removed by adding all chains of Coulomb interactions to form the screened potential, and finally the logarithmic divergence at short distance is removed by adding watermelons (or ladders) of screened interactions to bring in the distance of closest

approach $\beta e^2$ as the cutoff distance. The result is

$$\beta(F-F_0)=-\tfrac{1}{2}N^2\Big\{\int_0^1\frac{dc}{c}\int\frac{Vd^3k}{(2\pi)^3}\frac{(\beta u_c(k))^2}{1+N\beta u_c(k)}$$
$$+\sum_{m=3}\frac{(-\beta)^m}{m!}\int\cdots\int\frac{V^{m-1}d^3k_1\cdots d^3k_m}{(2\pi)^{3(m-1)}}$$
$$\times\delta(\mathbf{k}_1+\cdots+\mathbf{k}_m)\frac{u(k_1)}{1+N\beta u(k_1)}\cdots\frac{u(k_m)}{1+N\beta u(k_m)}\Big\} \quad (10a)$$

or as a configuration space integration

$$\beta(F-F_0)=-\tfrac{1}{2}N\rho\Big\{\beta^2\int_0^1\frac{dc}{c}\int d^3r\,u_c(r)u_{s,c}(r)$$
$$+\int d^3r[\exp[-\beta u_s(r)]-1+\beta u_s-\tfrac{1}{2}(\beta u_s)^2]\Big\}. \quad (10b)$$

The diagrams for $g(r)$ are obtained from those in Fig. 1 by the process of cutting the interaction between *every* pair of particles. The differentiation with respect to the coupling constant to give the internal energy, Eqs. (6) and (7), does this cutting.

Using the wave-number integral form of the free energy Eq. (10a) one finds

$$\beta(E-E_0)=-\tfrac{1}{2}N^2\Big\{\beta^2\int\frac{Vd^3k}{(2\pi)^3}u(k)u_s(k)$$
$$+\sum_{m=3}\frac{(-\beta)^m}{m!}\int\cdots\int\frac{V^{m-1}d^3k_1\cdots d^3k_m}{(2\pi)^{3(m-1)}}$$
$$\times\delta(\mathbf{k}_1+\cdots+\mathbf{k}_m)m\Big[c\frac{\partial}{\partial c}\frac{u_c(k)}{1+N\beta u_c(k)}\Big]_{c=1}$$
$$\times u_s(k_2)\cdots u_s(k_m)\Big\}. \quad (11)$$

The quantity in square brackets in Eq. (11) is

$$c\frac{\partial}{\partial c}u_{s,c}(k)\big|_{c=1}=\frac{u(k)}{[1+N\beta u(k)]^2}$$
$$=u(k)\Big[1-\frac{2N\beta u(k)}{1+N\beta u(k)}+\Big(\frac{N\beta u(k)}{1+N\beta u(k)}\Big)^2\Big] \quad (12)$$
$$=u(k)[1-2N\beta u_s(k)+(N\beta u_s(k))^2].$$

In the case of interest where $u(r)=e^2/r$ and $u(k)=4\pi e^2/Vk^2$, the correction factor in Eq. (12) arising from cutting every Coulomb line in the chains forming the screened potential is

$$(1+N\beta u(k))^{-2}=k^4/(k^2+\lambda_D^{-2})^2. \quad (13)$$

This correction factor has been broken into three parts in the second line of Eq. (12) in order to show correspondence with the diagrams for $g(r)$ or $g(k)$ in Fig. 2. Next by working directly from the diagrams of Fig. 2 or by using Eqs. (11) and (7) one finds for $g(k)$

$$g(k)=-\beta u_s(k)+[1-2N\beta u_s(k)+(N\beta u_s(k))^2]\times[h_2(k)+G_3(k)], \quad (14)$$

where

$$h_2(k)=\frac{\beta^2}{2!}\int\frac{d^3r}{V}\Big(\frac{e^2}{r}e^{-r/\lambda_D}\Big)^2e^{i\mathbf{k}\cdot\mathbf{r}}=\frac{4\pi(\beta e^2)^2}{2!Vk}\times\tan^{-1}k\lambda_D/2 \quad (15)$$

$$G_3(k)=\int\frac{d^3r}{V}e^{i\mathbf{k}\cdot\mathbf{r}}(e^{-\beta u_s}-1+\beta u_s-\tfrac{1}{2}(\beta u_s)^2)$$
$$=_{k=0}(4\pi\lambda_D^3/V)\times\{(\Lambda^3/3!)(\ln 3\Lambda+2c-11/6)\cdots\}. \quad (16)$$

The $m=3$ term in Eq. (11) has been separated from the $m>3$ terms [$h_2(k)$ and $G_3(k)$ in Eq. (14)] because of the fortunate circumstance that $1/r^2$ has a Fourier transform Eq. (15) whereas $1/r^n$ with $n>2$ does not. The Fourier transform of ladders of screened potentials $G_3(k)$ could be worked out completely, but since it is not needed it will not be given here.

Let us now introduce the dimensionless wave number $\kappa=k\lambda_D$ and the plasma parameter $\Lambda$ so that Eq. (14) may be written as[7]

$$g(k)=g(\Lambda,\kappa)_{\text{ring}}+g_{2,2}(\Lambda,\kappa)+g_{2,3+}(\Lambda,\kappa)\cdots$$
$$=\frac{4\pi\lambda_D^3}{V}\Big\{-\frac{\Lambda}{\kappa^2+1}+\frac{\kappa^4}{(\kappa^2+1)^2}\times\Big[\frac{\Lambda^2}{2!\kappa}\tan^{-1}\kappa/2+G_3(\Lambda,\kappa)\Big]\cdots\Big\}. \quad (17)$$

The notation $g_{2,2}$ means diagrams with two nodal points

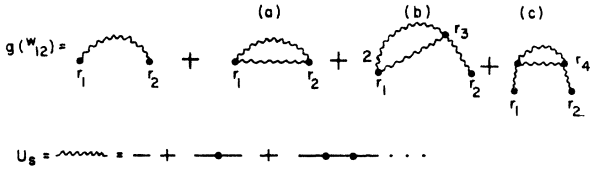


FIG. 2. Diagrams for the pair distribution function. The wavy lines indicate the Debye screened potential obtained by summing chains of Coulomb interactions as in Fig. 1. The labeling a, b, and c indicates the three diagrams one gets when the screened potential is cut in every possible way.

[7] The result for $g_{2,2}(k)$ was obtained independently by J. Coste (private communication).

and two screened potentials between them; $g_{2,3+}$ indicates two nodal points connected by three or more screened potentials. The sum $g_2(\Lambda,x)=g_{2,2}+g_{2,3+}$ in Eq. (7) gives the entire Abe $S_2(\Lambda)$ term of the free energy.

It is now convenient to divide up $g_{2,2}$ into a sum of three pieces,

$$g_{2,2}=g_{2,2}{}^a+g_{2,2}{}^b+g_{2,2}{}^c,$$

as indicated by the second line of Eq. (12) and the three diagrams shown in Fig. 2 resulting from the different ways of cutting the Coulomb interactions in the chains forming $u_s$. If to all orders in $\Lambda$ we take only diagrams of type a and neglect types b and c [thus replacing the correction factor $k^4/(k^2+\lambda_D{}^{-2})^2$ by 1] then we obtain

$$g_2{}^a(r)=g_{2,2}{}^a+g_{2,3+}{}^a=\sum_{m=2}[(-\beta u_s)^m/m!]$$
$$=\exp(-\beta u_s)-1+\beta u_s, \quad (18)$$

so that the complete pair distribution function to this approximation is

$$g(r)\approx 1+g_{\text{ring}}+g_2{}^a=\exp(-\beta u_s), \quad (19)$$

which is the nonlinear Debye-Hückel result. In the limit of zero density for which $u_s(r)\to e^2/r$, the nonlinear Debye-Hückel result reduces to the familiar Boltzmann factor. The terms $g_2{}^b=g_{2,2}{}^b+g_{2,3+}{}^c$ and $g_2{}^c=g_{2,2}{}^c+g_{2,3+}{}^c$ are corrections to the physically reasonable Boltzmann factor with $u_s(r)$ replacing $u(r)$.

Before proceeding with the exact calculation of $g_{2,2}{}^b$ and $g_{2,2}{}^c$ in configuration space a few general observations are in order. Since there are two fundamental lengths $\beta e^2$ and $\lambda_D$, there are three regions of $r$ to consider, $0<r<\beta e^2$, $\beta e^2<r<\lambda_D$, and $\lambda_D<r$. We observe that $g_{2,2}{}^a(r)$ goes as $(\beta e^2/r)^2$ for $r<\lambda_D$ and thus it is a reasonable correction to the Debye-Hückel term for $r>\beta e^2$, but for small $r$, i.e., less than $\beta e^2$, one must take the entire sum of ladders $g_2{}^a=g_{2,2}{}^a+g_{2,3+}{}^a$ to get the correct Boltzmann factor. The next correction $g_{2,2}{}^b$ is negative and goes as $1/k^3$ for large $k$ and hence as $\Lambda^2\ln(\lambda_D/r)$ for small $r$. Thus $g_{2,2}{}^b(r)$ is useful by itself only for $r>\beta e^2$ because of its logarithmic divergence as $r\to 0$; adding the remaining piece $g_{2,3+}{}^b(r)$ will remove this logarithmic divergence. The last correction $g_{2,2}{}^c$ is positive and goes as $1/k^5$ for large $k$ and hence $g_{2,2}{}^c(r)$ goes to a constant as $r\to 0$.

## III. EVALUATION OF $g_2(r)$ TO $O(\Lambda^2)$

Since $g_{2,2}$ is known exactly in $k$ space, as given by Eq. (17), we now need only to perform the Fourier inversion to find $g_{2,2}(r)$. The contribution from diagram (a) in Fig. 2 is

$$g_{2,2}{}^a(\Lambda,x)=(\Lambda^2/2!)(e^{-2x}/x^2). \quad (20)$$

The correction $g_{2,2}{}^b$ from Eq. (17) is

$$g_{2,2}{}^b(\Lambda,x)=\frac{(-2)(\beta e^2)^2}{2!}\int\frac{d^3k\,e^{i\mathbf{k}\cdot\mathbf{r}}}{(2\pi)^3}\frac{\lambda_D{}^{-2}}{k^2+\lambda_D{}^{-2}}\times\frac{\tan^{-1}k\lambda_D/2}{k}$$
$$=\frac{(-2)\beta^3\rho}{2!}\int d^3r_3 u_s(r_{23})(u_s(r_{13}))^2,\qquad r=r_{12}=|\mathbf{r}_1-\mathbf{r}_2|$$
$$=((-2)\Lambda^2/2!)(2x)^{-1}\times\{e^{-x}\ln 3-e^{-x}E_1(x)+e^xE_1(3x)\}, \quad (21)$$

where

$$E_1(x)=\int_x^\infty\frac{dy}{y}e^{-y}$$
$$=\ln(x\gamma)^{-1}-x+x^2/2.2!-\cdots, \quad x<1, \quad \gamma=e^c,$$
$$=(e^{-x}/x)(1-x^{-1}+2!/x^2-\cdots), \quad x>1. \quad (22)$$

For $x<1(r<\lambda_D)$ the expression for $g_{2,2}{}^b$ from Eq. (21) becomes

$$g_{2,2}{}^b(\Lambda,x)=\frac{(-2)\Lambda^2}{2!}\frac{\sinh x}{x}\ln\frac{1}{3\gamma x}, \quad (23)$$

and for $x>1$ it is

$$g_{2,2}{}^b(\Lambda,x)=-\frac{\Lambda^2}{2!}\left\{\frac{e^{-x}}{x}\ln 3-\frac{2}{3}\frac{e^{-2x}}{x^2}\right\}. \quad (24)$$

Note from Eq. (22) that the short-distance form of $g_{2,2}{}^b(\Lambda,x)$ is logarithmically divergent as anticipated in Sec. II. This logarithmic divergence is easily removed by adding the higher order terms indicated by $g_{2,3+}{}^b$. For $r=0$ one finds

$$g_2{}^b(r=0)=g_{2,2}{}^b+g_{2,3+}{}^b=-\Lambda^2\{\ln(1/\Lambda)-(\ln 3+2C-3/2)\}. \quad (25)$$

The final correction of $O(\Lambda^2)$- namely $g_{2,2}{}^c(\Lambda x)$- is

$$g_{2,2}{}^c(\Lambda,x)=\frac{(\beta e^2)^2}{2!}\int\frac{d^3k e^{i\mathbf{k}\cdot\mathbf{r}}}{(2\pi)^3}\frac{\lambda_D{}^{-4}}{(k^2+\lambda_D{}^{-2})^2}\times\frac{\tan^{-1}k\lambda_D/2}{k}$$
$$=\frac{\beta^4\rho^2}{2!}\int\int d^3r_3\,d^3r_4\,u_s(r_{13})u_s(r_{31})^2u_s(r_{42})$$
$$=(\Lambda^2/2!)(4x)^{-1}\{(1+x)e^{-x}\ln 3-\tfrac{4}{3}(e^{-x}-e^{-2x})-(1+x)e^{-x}E_1(x)+(1-x)e^xE_1(3x)\}. \quad (26)$$

For $x\ll 1$, Eq. (26) gives

$$g_{2,2}{}^c=(\Lambda^2/2!)\{\tfrac{1}{6}+\tfrac{1}{8}x\ln(3\gamma x)^{-1}\} \quad (27)$$

which is finite at $x=0$, and consequently $g_{2,3+}{}^c$ is not

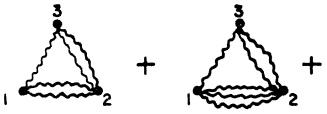


FIG. 3. Lowest order diagrams contributing to the three-node function $S_3(\Lambda)$. The structure connecting points 1 and 2 through 3 is $g_{2,2}{}^b$. The screened potentials connecting 1 and 2 directly give $\exp(-\beta u_s)-1+\beta u_s$. Cutting each of these screened lines gives the contribution $[\exp(-\beta u_s)-1]g_{2,2}{}^c$ to $g(r)$.

needed. Of more interest is the behavior of $g_{2,2}{}^c$ for $x>1$ ($r>\lambda_D$). The dominant term in Eq. (26) is evidently $e^{-x}\ln 3$, *which is larger than the Debye-Hückel term as* $x\to\infty$. The complete result for $g(r)$ to $O(\Lambda^2)$ for large $x$ is

$$g(r)=1-(\Lambda/x)e^{-x}+\tfrac{1}{8}\Lambda^2[e^{-x}\ln 3-(\tfrac{4}{3}+3\ln 3)\times(e^{-x}/x)]. \quad (28)$$

$g_2$ becomes larger than $g_{\text{ring}}$ when $x\gtrsim 8/(\Lambda\ln 3)$ even though $g_2$ is higher order in the coupling parameter $\Lambda$. This same phenomenon has been seen previously and more dramatically in the related problem of collision damping of plasma oscillations studied by DuBois, Gilinsky, and Kivelson.[8] For the electron gas the collisional damping in the long-wave limit (small $k$) is proportional to $\Lambda k^2$ while the lower order Landau damping in the same limit disappears as $\exp(-1/k^2)$.

We have seen that $g_2{}^b$ and $g_2{}^c$ are, respectively, $O(\Lambda^2\ln\Lambda)$ and $O(\Lambda^2)$ as $x\to 0$. This does not mean that $g(r)$ has a finite value of $O(\Lambda^2\ln\Lambda)$ at $r=0$, since in fact $g_2{}^b$ and $g_2{}^c$ are themselves multiplied by the Boltzmann factor $\exp(-\beta u_s)$ which goes rapidly to zero as $r\to 0$. The derivation of the Boltzmann factor with the screened potential Eqs. (18) and (19) required only the watermelon diagrams giving the Abe $S_2(\Lambda)$ function. An examination of the diagrams which make up the three-node term $S_3(\Lambda)$ shows as indicated in Fig. 3 that $g_2{}^b$ is included in some of the diagrams. Such diagrams may be looked at as a special case of the watermelon diagrams connecting two nodal points except that one screened interaction $-\beta u_s$ is replaced with $g_2{}^b(\Lambda,x)$. From these diagrams one obtains a contribution to the pair distribution function of the form $[\exp(-\beta u_s)-1]g_2{}^b$. Similarly in the diagrams for $S_4(\Lambda)$ one finds $g_2{}^c(\Lambda,x)$ and a contribution to $g(r)$ of the form $[\exp(-\beta u_s)-1]g_2{}^c$. Adding these contributions to $g_2{}^b$ and $g_2{}^c$ obtained from $S_2(\Lambda)$, one gets the complete Boltzmann factor. This same argument holds for any correction to $g(r)$ of some power of $\Lambda$ obtained from the diagrams for $S_n(\Lambda)$ for some $n$; the same structure will be found in diagrams of larger $n$ and will result in the given piece being multiplied by the Boltamann factor. Thus a practical expression for $g(r)$ valid from $r=0$ to $\infty$ and which is exact to $O(\Lambda^2)$ for $r>\beta e^2$ is

$$g(r)=e^{-\beta u_s}\{1+g_2{}^b(r)+g_{2,2}{}^c(r)\}, \quad (29)$$

where $g_2{}^b(r)$ is adequately approximated by $g_{2,2}{}^b$ from Eq. (21) for $r>\beta e^2$. $g_2{}^b(r)$ is negative for all $r$ and $g_{2,2}{}^c(r)$ is positive for all $r$. The factor in braces multiplying the Boltzmann factor in Eq. (29) reduces the pair distribution function below $\exp(-\beta u_s)$ for $0<r<\lambda_D$ and $g_{2,2}{}^c(r)$ dominates for large $r$, $r\gg\lambda_D$. A plot of $g(r)$ as given by Eq. (29) is shown in Fig. 4.

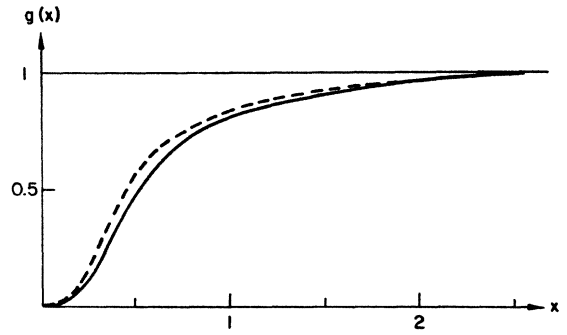


FIG. 4. Plot of $g(r)$ from Eq. (29) for $\Lambda=0.5$. The dashed line shows for comparison the result from the Boltzmann factor $\exp(-\beta u_s)$.

*Note added in proof.* Recently it has come to the author's attention that most of the results of this paper have been obtained independently several times. Although some of the earlier investigations have been published, the results for $g(r)$ beyond the Debye expression do not seem to be well known, perhaps because the original publications were in Russian. Results have been obtained by Tyablikov and Tolmachev,[9] Fisher,[10] Hooper, Jr.,[11] Coste,[12] Hirt,[13] and O'Neil and Rostoker.[14] References 9, 10, 12, and 14 use the Bolgoliubov hierarchy of equations for the distribution functions while Refs. 11 and 13 use the Abe diagrammatic expansion technique. The present paper differs from Refs. 11 and 13 only in that the diagrammatic method begins with the free energy expansion to obtain the results for $g(r)$.

## ACKNOWLEDGMENT

The author wishes to thank Dr. Philippe de Gottal and Dr. Radu Balescu for several useful conversations concerning this work, and also acknowledges the hospitality of Professor I. Prigogine of the Universite Libre in Brussels where this work was begun.

[8] D. F. DuBois, V. Gilinsky, and M. G. Kivelson, Phys. Rev. **129**, 2376 (1963).

[9] S. V. Tyablikov and V. V. Tolmachev, Dokl. Akad. Nauk SSSR **114**, 1210 (1957) [English transl.: Soviet Phys.—Doklady 2, 299 (1957)].

[10] I. Z. Fisher, *Statistical Theory of Liquids* (University of Chicago Press, Chicago, 1964), pp. 109–118.

[11] C. F. Hooper, Jr., Ph.D. thesis, Department of Physics, Johns Hopkins University, 1963 (unpublished).

[12] J. Coste (unpublished).

[13] C. W. Hirt, Phys. Fluids **8**, 693 (1965).

[14] T. O'Neil and N. Rostoker, Phys. Fluids **8**, 1109 (1965).